Progress In Electromagnetics Research M, Vol. 32, 83–93, 2013

ANALYSIS OF NOVEL FRACTAL OPTICAL ANTENNA ARRAYS — A CONCEPTUAL APPROACH

Mounissamy Levy [1, 2, *], Dhamodharan S. Kumar [2], and Anh Dinh [1]

[1]Department of Electrical and Computer Engineering, University of Saskatchewan, Saskatoon S7N 5A9, Canada

[2]Department of Electronics and Communication Engineering, National Institute of Technology, Tiruchirappalli 620015, India

Abstract—This paper presents the analysis of novelistic fractal optical antenna arrays in a conceptual manner. Fractal antennas are array antennas with converging and diverging growth of basic element or elements for multi-wideband capturing of the electromagnetic waves. Most of these antennas relay on two components for their characteristics. First one is the basic stage shape and second one is the number of stages of growth. For computing the direction of radiation the well-defined fractal array manifold and a good estimate of the covariance matrix of the fractal array response is needed.

1. INTRODUCTION

FRACTAL THEORY is a relatively emerging field of mathematics that has changed the way scientists view of looking at a natural occurring phenomena in this world [1–9]. This paper makes an attempt of extending the concept of fractal antenna array to the optical regime for the design of fractal optical antenna arrays. Being seen as a breakthrough technology, free space optics system has stringent requirements for the design of the optical antenna. An optical antenna has many characteristics for its performance measurement. Some of the figures of merit for optical antennas includes impedance of a nano antenna such as a vacuum, a micro cavity, a dipolar nano antenna, plasmonic antenna and antenna array, comparison of a micro cavity and nano antenna, its ohmic and radiative losses, the impedance of a quantum emitter, two level system impedance

Received 13 May 2013, Accepted 20 July 2013, Scheduled 29 July 2013

* Corresponding author: Mounissamy Levy (levy_young@yahoo.com).

and multiple scattering, properties of coated nano particles, field enhanced spectroscopy, directionality, polarization and enhancement, quantum optics and near field microscopy, nonlinear optical antenna characteristics and coherent control of nano particle excitations. The explosive growth of free space optic communication devices, and their importance in all aspects of our lives, made a growing need to develop portable and higher data rate free space optic components. A vital role is played by optical antenna in this regard. For next generation devices, the need for optic antennas and free space optic front-ends, without compromising performance, has emerged as a key driver in marketing and realizing. Several new applications utilizing the optical frequency range have been evolved, and new antennas have been designed and tested. In this paper, novel fractal optical antenna arrays are analyzed in a conceptual manner. The paper is arranged as follows. Section 2 highlights the analysis of the fractal antenna and novel fractal optical antenna array. Finally Section 3 concludes with the conclusion and gives some direction for future research.

2. NOVEL FRACTAL ANTENNA ANALYSIS AND A CONCEPTUAL APPROACH FOR FRACTAL OPTICAL ANTENNA ARRAYS

In the RF regime, for linear, time invariant, isotropic media,considering isotropic point source radiators, the time domain constitutive equation relating the electric field density $\bar{D}$ is typically cast as a convolution between $\bar{E}$ and the permittivity as follows[10]

$$\bar{D}(\bar{r},t) = \int_{-\infty}^{t} \epsilon(\bar{r},t-\tau)\bar{E}(\bar{r},\tau)d\tau \tag{1}$$

$$\epsilon(\bar{r},t) = \epsilon_0\delta(t) + \epsilon_0\chi_e(\bar{r},t) \tag{2}$$

where $\epsilon(\bar{r},t) = F^{-1}[\epsilon(\bar{r},\omega)]$ is the time domain permittivity function, and F stands for Fourier transformation. ϵ_0 is the vacuum permittivity, $\delta(t)$ the Dirac delta function, and $\chi_e(\bar{r},t)$ the time domain electric susceptibility function. In FDTD or FETD, the time variable is discretized as $t_l = l\Delta t$ with $= 0, 1, 2 \ldots$. We denote

$$\bar{E}(l\Delta t) = \bar{E}^l \tag{3}$$

From which we can write

$$\sum_{p=0}^{N_1} a_p(\bar{r}) \frac{\partial^p \bar{D}(\bar{r},t)}{\partial t^p} = \sum_{p=0}^{N_2} b_p(\bar{r}) \frac{\partial^p \bar{E}(\bar{r},t)}{\partial t^p} \tag{4}$$

where $a_p(\bar{r})$ and $b_p(\bar{r})$ equate the relation between dielectric constant, flux density and electric field intensity. The Maxwell's equation relates

the electric field intensity and the magnetic flux density given by

$$\nabla_s \times \bar{E} = j\omega\bar{B} \tag{5}$$

and the magnetic field intensity, electric flux density and electric field by the following equation

$$\nabla_s \times \bar{H} = -j\omega\bar{D} + \sigma\bar{E} \tag{6}$$

where

$$\nabla_s = \hat{x}\frac{1}{s_x}\frac{\partial}{\partial x} + \hat{y}\frac{1}{s_y}\frac{\partial}{\partial y} + \hat{z}\frac{1}{s_z}\frac{\partial}{\partial z} \tag{7}$$

and s_i denotes

$$s_i = a_i + j\Omega_i, \quad i = x, y, z \tag{8}$$

From Equation (7)

$$\frac{1}{s_x}\frac{\partial}{\partial x}\hat{x} \times \bar{E} = j\omega\bar{B}_{sx} \tag{9}$$

$$\frac{1}{s_x}\frac{\partial}{\partial x}\hat{x} \times \bar{H} = -j\omega\bar{D}_{sx} + \sigma\bar{E}_{sx} \tag{10}$$

$$\frac{\partial}{\partial x}\hat{x} \times \bar{E} = j\omega a_x\bar{B}_{sx} - \Omega_x\bar{B}_{sx} \tag{11}$$

A fractal is a recursively generated object having a fractional dimension. Many objects, including antennas, can be designed using the recursive nature of a fractal. The important properties of fractal arrays are frequency independent multi band characteristic schemes for realizing low side-lobe designs, systematic approaches to thinning, and the ability to develop rapid beam-forming algorithms by exploiting the recursive nature of fractals. These arrays have fractional dimensions that are found from generating sub array used to recursively create the fractal array. Repetitive application of a generating sub array can form a rich class of fractal array. A generating sub array is a small array at scale one ($P = 1$) where P is the scale factor and used to construct larger arrays of higher scales ($P > 1$). The generating sub array elements are turned on and off in a particular pattern in many cases. A set of formulas for copying, scaling, and translation of the generating sub array are then followed in order to produce the fractal array. Hence, fractal arrays created in this manner will be composed of a sequence of self-similar sub arrays. In other words, this may be conveniently considered as an array of arrays. The array factor for a fractal array [6] of this type may be expressed in the general form:

$$AF_P(\psi) = \prod_{i=1}^{P} \hat{G}A\left(\delta^{i-1}\psi\right) \tag{12}$$

where $GA(\psi)$ represents the array factor associated with the generating sub array. The parameter δ is a scale or expansion factor that governs how large the array grows with each recursive application of the generating sub array. The expression for the fractal array factor given in Equation (12) is simply the product of scaled versions of a generating sub array factor. Therefore, Equation (12) may be regarded as representing a formal statement of the pattern multiplication theorem for fractal arrays.

For the novel fractal antenna, as the number of stages P is varied, the size of the fractal element also varies i.e., the δ value also changes. For analysis purpose, we will introduce the parameter 'x' which indicates the size increase proportion. In the case of diverging growth, the value of 'x' is greater than unity, and in the case of converging growth, the 'x' value is less than unity. The larger is the value of 'x', the higher will be the growth. Implementing this change in the equations above for $P = 1$ and $\delta = 1$, the equations become

$$\frac{1}{s_{x1,1x}}\frac{\partial}{\partial_{x1,1x}}\hat{x} \times \bar{E}_{1,1x} = j\omega\bar{B}_{sx1,1x} \tag{13}$$

$$\frac{1}{s_{x1,1x}}\frac{\partial}{\partial_{x1,1x}}\hat{x} \times \bar{H}_{1,1x} = -j\omega\bar{D}_{sx1,1x} + \sigma\bar{E}_{sx1,1x} \tag{14}$$

$$\frac{\partial}{\partial_{x1,1x}}\hat{x} \times \bar{E}_{1,1x} = j\omega a_{x1,1x}\bar{B}_{sx1,1x} - \Omega_{x1,1}\bar{B}_{sx1,1x} \tag{15}$$

These equations can be extended to find the magnetic field intensity from the electric field intensity and the electric flux density by the following equation. Since the antenna is fabricated in the same substrate and material, everything else remains constant only the fields produced by each growth will vary

$$\begin{aligned}\frac{\partial}{\partial_{x1,1x}}\hat{x} \times \bar{H}_{x1,1x} &= -j\omega a_{x1,1x}\bar{D}_{sx1,1x} + \Omega_{x1,1x}\bar{D}_{sx1,1x} + a_{x1,1x}\sigma\bar{E}_{sx1,1x} \\ &\quad + j\frac{\Omega_{x1,1x}}{\omega}\sigma\bar{E}_{sx1,1x} \end{aligned} \tag{16}$$

$$\frac{\partial}{\partial_{x1,1x}}\hat{x} \times \bar{E}_{x1,1x} = -a_{x1,1x}\frac{\partial}{\partial t}\bar{B}_{sx1,1x} - \Omega_{x1,1x}\bar{B}_{sx1,1x} \tag{17}$$

$$\begin{aligned}\frac{\partial}{\partial_{x1,1x}}\hat{x} \times \bar{H}_{x1,1x} &= a_{x1,1x}\frac{\partial}{\partial t}\bar{D}_{sx1,1x} + \Omega_{x1,1x}\bar{D}_{sx1,1x} + a_{x1,1x}\sigma\bar{E}_{sx1,1x} \\ &\quad + \Omega_{x1,1x}\sigma\int_0^t \bar{E}_{sx1,1x}(\tau)d\tau \end{aligned} \tag{18}$$

The magnetic field intensity and the magnetic flux density are related by

$$\bar{B}_{sx1,1x} = \mu\bar{H}_{sx1,1x} \tag{19}$$

Similarly the electric field intensity and the electric flux density are related by

$$\bar{D}_{sx1,1x} = \epsilon\,(t) *_t \bar{E}_{sx1,1x} \tag{20}$$

The electric permittivity in time domain is related to the electric susceptibility of the medium in frequency domain by the Fourier inverse function given by

$$\epsilon(t) = \mathcal{F}^{-1}[\epsilon(\omega)] \tag{21}$$

where $\epsilon(t)$ is the N-species Lorentzian dispersive medium given by the following frequency-dependent relative permittivity function

$$\epsilon(\omega) = \epsilon_0[\epsilon_\infty + \chi(\omega)] \tag{22}$$

$$\epsilon_0\epsilon_\infty + \epsilon_0(\epsilon_s{-}\epsilon_\infty) \sum_{m=1}^{N} \frac{G_m\omega_m^2}{\omega_m^2 - j2\omega\alpha_m - \omega^2} \tag{23}$$

where ϵ_0 and ϵ_∞ are the static and infinite frequency permittivities, and ϵ_s is the permittivity for the given values. An equivalent time domain susceptibility function can be defined by

$$\hat{\chi}(t) = \sum_{m=1}^{N} \hat{\chi}_m(t) = \sum_{m=1}^{N} j\gamma_m e^{-(\alpha_m + j\beta_m)} u(t) \tag{24}$$

where

$$\beta_m = \sqrt{\omega_m^2 - \alpha_m^2} \tag{25}$$

And

$$\gamma_m = (\epsilon_s{-}\epsilon_\infty)\frac{G_m\omega_m^2}{\beta_m} \tag{26}$$

Note that the limit value for G_m is unity which is a normalized quantity.

$$\sum_{m=1}^{N} G_m = 1 \tag{27}$$

the electric flux density for the proposed fractal antenna is given by

$$\bar{D}_{x1,1x}(t) \;=\; \epsilon_0\epsilon_\infty \bar{E}_{x1,1x}(t) + \epsilon_0\chi_{x1,1x}\,(t) *_t \bar{E}_{x1,1x}(t) \tag{28}$$

$$\bar{D}_{x1,1x}(t) \;=\; \epsilon_0\epsilon_\infty \bar{E}_{x1,1x}\,(t) + \epsilon_0 \sum_{m=1}^{N} \mathrm{Re}\{\hat{\chi}_{x1,1x}\,(t) *_t \bar{E}_{x1,1x}(t)\} \tag{29}$$

The electric field at $t = l\Delta_t$ using piecewise-linear approximation for the time discretization can be written as

$$\bar{E}\,(t) = \bar{E}^l + \frac{t - l\Delta_t}{\Delta_t}\left(\bar{E}^{l+1} - \bar{E}^l\right) \tag{30}$$

When substituted we get,

$$\bar{D}^l = \epsilon_0 \epsilon_\infty \bar{E}^l + \epsilon_0 \sum_{m=1}^{N} \mathrm{Re}\{\bar{Q}_m^l\} \tag{31}$$

where

$$\bar{Q}_m^l = \sum_{p=0}^{l-1} \left[\left(\hat{\chi}_m^0 - \hat{\zeta}_m^0 \right) \bar{E}^{l-p} + \hat{\zeta}_m^0 \bar{E}^{l-p-1} \right] e^{-(\alpha_m + j\beta_m)p\Delta_t} \tag{32}$$

With the constants given by $\hat{\chi}_m^0 = \int_0^{\Delta_t} \hat{\chi}_m(t)dt = \frac{j\gamma_m}{(\alpha_m + j\beta_m)} \{1 - e^{-(\alpha_m + j\beta_m)\Delta_t}\}$

$$\begin{aligned} \hat{\zeta}_m^0 \;&=\; \int_0^{\Delta_t} t\hat{\chi}_m(t)\, dt = \frac{j\gamma_m}{\Delta_t(\alpha_m + j\beta_m)^2} \\ &\left\{ 1 - \left[((\alpha_m + j\beta_m)\Delta_t + 1) \right] e^{-(\alpha_m + j\beta_m)\Delta_t} \right\} \end{aligned} \tag{33}$$

The following recursive calculation can be carried out for determining $\bar{Q}_m^l$

$$\bar{Q}_m^l = \begin{cases} 0 & l = 0 \\ \left(\hat{\chi}_m^0 - \hat{\zeta}_m^0 \right) \bar{E}^l + \hat{\zeta}_m^0 \bar{E}^{l-1} + \bar{Q}_m^{l-1} e^{-(\alpha_m + j\beta_m)\Delta_t} & l \geq 0 \end{cases} \tag{34}$$

After substituting this into electric flux density the equation becomes

$$\begin{aligned} \bar{D}^l \;&=\; \epsilon_0 \left(\epsilon_\infty + \sum_{m=1}^{N} \mathrm{Re}\left(\hat{\chi}_m^0 - \hat{\zeta}_m^0 \right) \right) \bar{E}^l + \epsilon_0 \sum_{m=1}^{N} \mathrm{Re}\left(\hat{\zeta}_m^0 \right) \bar{E}^{l-1} \\ &+ \epsilon_0 \sum_{m=1}^{N} \mathrm{Re}\left(\bar{Q}_m^{l-1} e^{-(\alpha_m + j\beta_m)\Delta_t} \right) \end{aligned} \tag{35}$$

And simplified becomes

$$\bar{D}^l \;=\; \epsilon_0 \left(\lambda_0 \bar{E}^l + \lambda_1 \bar{E}^{l-1} + \bar{P}^{l-1} \right) \tag{36}$$

$$\lambda_0 \;=\; \left(\epsilon_\infty + \sum_{m=1}^{N} \mathrm{Re}\left(\hat{\chi}_m^0 - \hat{\zeta}_m^0 \right) \right) \tag{37}$$

and

$$\lambda_1 = \sum_{m=1}^{N} \mathrm{Re}\left(\hat{\zeta}_m^0 \right) \tag{38}$$

and

$$\bar{P}^{l-1} = \sum_{m=1}^{N} \mathrm{Re}\left(\bar{Q}_m^{l-1} e^{-(\alpha_m + j\beta_m)\Delta_t}\right) \tag{39}$$

All these equations pertain to a single element of a single stage. The same equations can be repeated for the other elements in single stage and all the elements in subsequent stages of growth with the subscripts changed. The total electric field is given by the vector addition of the electric field produced by the individual stages.

$$\bar{E}_{tot}(t) \approx \bar{E}_{x1,1x}(t) + \bar{E}_{x2,2x}(t) + \bar{E}_{x3,3x}(t) + \bar{E}_{x4,4x}(t) + \bar{E}_{x5,5x}(t) \tag{40}$$

The total electric flux density is given by

$$\bar{D}_{tot}(t) \approx \bar{D}_{x1,1x}(t) + \bar{D}_{x2,2x}(t) + \bar{D}_{x3,3x}(t) + \bar{D}_{x4,4x}(t) + \bar{D}_{x5,5x}(t) \tag{41}$$

This equation holds well as long as the distance between different stages of growth is so small so that it can be neglected in far field calculations. This is a proven numerical method. This analysis carried out in the RF regime can be applied to optical regime for the design of fractal optical antenna arrays carefully incorporating the similarities and differences mentioned below. The fractal antenna array factor pattern and the directivity pattern in the RF regime and optical regime fundamental mode of operation considering the linear array of isotropic point source radiators for $P \in \{1, 2, 3, 4\}$ and $\delta = \{3, 5, 7\}$ are shown in Figures 1 to 4 [6].

The design procedure and equations for designing antenna arrays in the optical regime has many similarities to the design of antenna

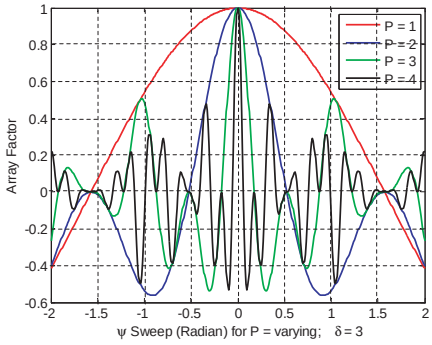

Figure 1. Combined fractal array factor pattern in the optical regime is the same as RF regime when operated in fundamental mode for $\delta = 3$.

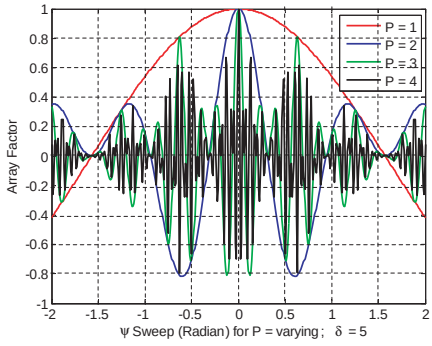

Figure 2. Combined fractal array factor pattern in the optical regime is the same as RF regime when operated in fundamental mode for $\delta = 5$.

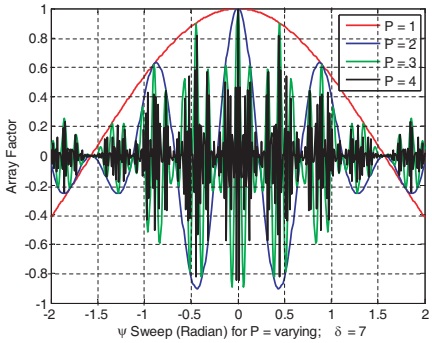

Figure 3. Combined fractal array factor pattern in the optical regime is the same as RF regime when operated in fundamental mode for $\delta = 7$.

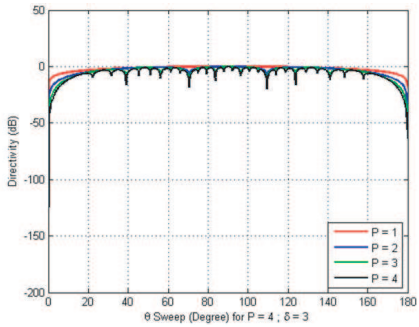

Figure 4. Combined fractal antenna directivity pattern in the optical regime is the same as RF regime when operated in fundamental mode.

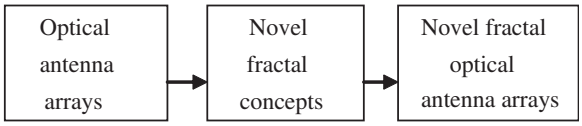

Figure 5. Block diagram of fractal optical antenna arrays.

array in the RF regime [11]. Figure 5 shows the block diagram of fractal optical antenna arrays. In the case of optical antenna array, the elements considered here are linear array of plasmonic dipoles. The fractal concept can be applied with the linear array. The basic Triadic cantor set can be followed in the case of linear array, or the Sierpinski carpet set can be followed in the case of planar array.

The most employed antenna element in the RF regime is the half wave length antenna. A RF antenna has its dipole resonance at a length of approximately half the free space wave length. However, the resonance length of an optical antenna is not dictated by the free space or vacuum wave length, but by the SPP (Surface Plasmon Polaritons) wavelength in the metal [11]. Considering the thickness of the wire used in an optical antenna, this expression changes. The electromagnetic fields are not required to vanish at the physical wire ends considering the boundary conditions in the case of RF. Their penetration into the surrounding medium leads to an additional phase that is picked up upon reflection. This is also known as apparent length increase of an antenna. Both effects lead to a substantial decrease of

the antenna resonance length. There are several ways of incorporating this difference into the array design of fractal optical antenna. The non-trivial method is to simulate the individual antenna elements first. This will take care of the apparent length increase effect and SPP wavelength effect. For cylindrical antennas, analytical expressions are derived to calculate the SPP wavelength of an infinitely long wire and the phase pickup upon reflection for an abruptly ending nano wire.

Yet another more subtle consequence is caused by the difference between SPP wavelength and free-space wavelength. Compared with the current distribution in wire antennas which results in standing wave pattern, the current in the optical antenna builds up a standing wave pattern similar to that of the RF antennas. However, the distance between the subsequent current lobes is not the same. Only when operated in fundamental mode, the emission pattern of the two antennas has nearly the same shape [11]. However, for higher mode of antenna operation, the different wavelengths can lead to fundamentally different emission patterns. Therefore, care has to be taken when the design of an antenna array that involves higher order resonance modes is shifted to optical regime wavelengths.

In the RF regime, the losses in antennas are mainly due to radiation damping. However, plasmonic currents in optical antennas also suffer from ohmic losses. Depending on the operation wavelength, the antenna efficiency decreases which cannot be ignored. For an antenna array consisting of only active elements, the effect will be less emitted radiation. But when an antenna array includes passive elements that are driven by the fields of active elements, adding further element can lead to a decrease of the antenna gain. A classic example is the Yagi-Uda antenna with an active feed element, a passive reflector and several passive directors. In the RF regime, the emitted power in the direction along the directors is enhanced when adding a second and third director. However, in the visible wavelength range, the losses in the Au elements lead to maximal radiation enhancement of an optical Yagi-Uda antenna with only one director [11].

State of the art nano fabrication techniques like EBL (Electron Beam Lithography) or FIB (Focussed Ion Beam) milling precisely pattern homogeneous nano structures in a 2D periodic arrangement. Similar to RF antenna arrays, plasmonic antenna arrays can achieve a higher directionality [11]. Application of the fractal concepts leads to further increasing the directivity, easily producing rapid beam forming algorithms, increasing the computational speed, enhancing the multiband operation and wider bandwidth with less computational complexity.

As with their RF counterparts, optical antennas have the ability

to focus free space radiation to a very small subwavelength volume with high field enhancements. Vice versa, coupling of a nanoscopic source, like quantum emitters, to an optical antenna results in modification of the transition rates and a redirection of the emission. Optical antenna arrays have superior properties regarding directivity, field confinement, absorption cross-section and flexibility in beam shaping compared with single plasmonic antennas. The future applications of optical antenna arrays are very interesting: nanoscale spectroscopy, efficient quantum light sources, and coherent control of field localization or high speed data transmission. However, current research is mainly focused on single optical antennas [11].

3. CONCLUSION

The diverging and converging fractal antennas are analyzed and studied, and the concept is extended to optical antenna arrays. The obtained analytical expressions are promising for future applications. The numerical method gives an insight to the mathematical analysis and the field values obtained. Further research can be continued with different basic cell shapes, and nonlinear array can be introduced to tailor the result according to the application requirements for challenging problems in fractal optical antenna arrays. In this case, the converging fractal structure is used in which case the fractal stage of growth converges as the growth approaches infinity. The other fractal structure is the diverging fractal concept in which the stage approaches infinity as the growth approaches infinity.

ACKNOWLEDGMENT

The primary author thanks the Canadian Government and Indian Government for the Award of Canadian Commonwealth Scholarship.

REFERENCES

1. Gianvittorio, J. P. and Y. Rahmat-Samii, "Fractal antennas: A novel antenna miniaturization technique, and applications," *IEEE Antennas and Propagation Magazine*, Vol. 44, No. 1, 20–36, Feb. 2002.
2. Best, S. R., "The fractal loop antenna: A comparison of fractal and non-fractal geometries," *IEEE Antennas and Propagation Society International Symposium*, Vol. 3, 146–149, 2001.
3. Werner, D. H. and S. Ganguly, "An overview of fractal antenna engineering research," *IEEE Antennas and Propagation Magazine*, Vol. 45, No. 1, 38–57, Feb. 2003.

4. Kim, Y. and D. L. Jaggard, "The fractal random array," *Proceedings of the IEEE*, Vol. 74, No. 9, 1278–1280, 1986.
5. Lakhtakia, A., N. S. Holter, and V. K. Varadan, "Self-similarity in diffraction by a self-similar fractal screen," *IEEE Transactions on Antennas and Propagation*, Vol. 35, No. 2, 236–239, Feb. 1987.
6. Werner, D. H., R. L. Haupt, and P. L. Werner, "Fractal antenna engineering: The theory and design of fractal antenna arrays," *IEEE Antennas and Propagation Magazine*, Vol. 41, No. 5, 37–58, Oct. 1999.
7. Liang, X., Z. Wu, and W. Wang, "Synthesis of fractal patterns from concentric-ring arrays," *IEEE Elec. Letters*, Vol. 32, No. 21, 1940–1941, Oct. 1996.
8. Puente Baliarda, C. and R. Pous, "Fractal design of multiband and low side-lobe arrays," *IEEE Transactions on Antennas and Propagation*, Vol. 44, No. 5, 730–739, May 1996.
9. Mandelbrot, B. B., *The Fractal Geometry of Nature*, W. H. Freeman and Company, New York, 1983, ISBN: 978-0716711865.
10. Gross, F. B., Editor-in-Chief., *Frontiers in Antennas: Next Generation Design & Engineering*, McGraw-Hill, New York, 2011.
11. Agio, M. and A. Alù, Editors, *Optical Antennas*, Cambridge University Press, New York, 2013.